



The Effect of Anisotropy on the Structure Optimization Using Golden-Section Search Algorithm Based on BEM

Mohamed Abdelsabour Fahmy^{1,2*}

¹Faculty of Computer and Informatics, Suez Canal University, New Campus, 4.5 Km, Ring Road, El Salam District, 41522 Ismailia, Egypt.

²Jamoum University College, Umm Al-Qura University, Alshohdaa 25371, Jamoum, Makkah, Saudi Arabia.

Author's contribution

The sole author designed, analyzed and interpreted and prepared the manuscript.

Article Information

DOI: 10.9734/JAMCS/2017/37822

Editor(s):

(1) Nikolaos Dimitriou Bagis, Professor, Department of Informatics and Mathematics, Aristotelian University of Thessaloniki, Greece.

Reviewers:

(1) Belkacem Chaouchi, Khemis Miliana University, Algeria.

(2) Francisco Bulnes, Technological Institute of High Studies of Chalco, Mexico.

Complete Peer review History: <http://www.sciedomains.org/review-history/21953>

Received: 30th October 2017

Accepted: 13th November 2017

Published: 17th November 2017

Original Research Article

Abstract

Aims: A shape optimization technique is developed, using the boundary element method, for two-dimensional anisotropic structures to study the effects of anisotropy on the displacements and stresses, then minimize weight while satisfying certain constraints upon stresses and geometry.

Study Design: Original Research Paper.

Place and Duration of Study: Jamoum University College, Mathematics Department, between June 2016 and July 2017.

Methodology: The shape design sensitivity analysis of a two-dimensional anisotropic structure using a singular formulation of the boundary element method is investigated to study the effects of anisotropy on the displacements and stresses. An Implicit differentiation technique of the discretized boundary integral equations is performed to produce terms that contain derivatives of the fundamental solutions employed in the analysis. This technique allows the coupling between optimization technique and numerical boundary element method (BEM) to form an optimum shape design algorithm that yields shape design sensitivities of the displacement and stress fields for anisotropic materials with very high accuracy. The fundamental solutions of displacements and tractions in terms of complex variables employed in the analysis. The feasible direction method was developed and implemented for use with the golden-section search algorithm based on BEM as a numerical optimization technique for minimizing weight while satisfying all of the constraints.

*Corresponding author: E-mail: mohamed_fahmy@ci.suez.edu.eg;

Results: The proposed method has been verified by using the two-dimensional plate with an elliptical hole as the numerical example. The numerical results show that the proposed method is suitable and effective tool for the computer implementation of the solution.

Conclusion: From the research that has been performed, it is possible to conclude that the optimal shape of the two-dimensional plate with an elliptical hole is crucial when elastic field is sensitive to boundary shape. Also from this knowledge of the effects of anisotropy on the displacements and stresses, we can design various anisotropic structures to meet specific engineering requirements and utilize within which to place new information can be more effective.

Keywords: Shape optimization; design sensitivity; implicit differentiation method; anisotropic structures; boundary element method.

2010 Mathematics subject classification: 65M38 - 65K05 - 74B05 - 74E05 - 74F05 - 74H05 - 74H15 - 74S20 - 90C31.

1 Introduction

The rapid development of composite materials following wide varieties of techniques and the design and manufacturing technologies is one of the most significant achievements in the field of materials engineering and science. Because of their high stiffness and high strength properties, composites are the most commonly used in mechanical engineering and aerospace applications [1-5].

In recent years, the scientific research in the field of optimization algorithms has become a rapidly developing area of research in computational optimization techniques [6-8].

Numerical techniques are also increasingly used for analysis of structural engineering, among which the boundary element technique [9-19], which offers a clear advantage over other methods, and is applicable to a wide range of structural engineering problems. The study of anisotropic structures is very complex and is still not well understood, and as a result, more sophisticated strategies for optimal design of anisotropic structure are in demand [20-25].

2 Formulation of the Problem

The equilibrium equation for anisotropic elasticity

$$\sigma_{ij,j} + X_j = 0 \quad (1)$$

where there are 21 independent material elastic constants C_{ijkl} because $C_{ijkl} = C_{jikl} = C_{ijlk} = C_{klij}$. Due to the symmetry of the stress and strain tensors, and assuming that the material is symmetric with respect to the z -direction which is perpendicular to $x - y$ plane, the two-dimensional stress-strain relations for plane-stress anisotropic elasticity are

$$\begin{bmatrix} \varepsilon_{xx} \\ \varepsilon_{yy} \\ \varepsilon_{xy} \end{bmatrix} = \begin{bmatrix} d_{11} & d_{12} & d_{16} \\ d_{12} & d_{22} & d_{26} \\ d_{16} & d_{26} & d_{66} \end{bmatrix} \begin{bmatrix} \sigma_{xx} \\ \sigma_{yy} \\ \sigma_{xy} \end{bmatrix} \quad (2)$$

where σ_{ij} and ε_{ij} ($i, j = x, y$) are the stress and strain components, respectively, d_{pq} are the elastic compliances coefficients, which can be written in terms of elastic constants as follows

$$\begin{aligned} d_{11} &= \frac{1}{E_1}, d_{22} = \frac{1}{E_2}, a_{12} = -\frac{\nu_{12}}{E_1} = -\frac{\nu_{21}}{E_2} \\ d_{66} &= \frac{1}{\mu_{12}}, \quad d_{16} = \frac{\eta_{12,1}}{E_1} = \frac{\eta_{1,12}}{\mu_{12}}, d_{26} = \frac{\eta_{12,2}}{E_2} = \frac{\eta_{2,12}}{\mu_{12}} \end{aligned} \quad (3)$$

The coefficients of mutual influence of the first and second kinds, respectively

$$\begin{aligned} c_{pq} &= d_{pq} - \frac{d_{p3}d_{q3}}{d_{33}}, \quad p, q = 1, 2, 6 \\ d_{p3} &= -\frac{\nu_{p3}}{E_p}, d_{33} = \frac{1}{E_3}, d_{63} = \frac{\eta_{12,3}}{E_3} = \frac{\eta_{3,12}}{\mu_{12}} \end{aligned} \quad (4)$$

The strain compatibility equation is

$$\frac{\partial^2 \varepsilon_{11}}{\partial x_2^2} + \frac{\partial^2 \varepsilon_{22}}{\partial x_1^2} = 2 \frac{\partial^2 \varepsilon_{12}}{\partial x_1 \partial x_2} \quad (5)$$

The equilibrium equation is automatically satisfied by writing the stresses in terms of derivatives of the Airy stress function $\phi(x_1, x_2)$ proposed by Airy [26] as

$$\sigma_{11} = \frac{\partial^2 \phi}{\partial x_2^2}, \sigma_{22} = \frac{\partial^2 \phi}{\partial x_1^2}, \sigma_{12} = \frac{\partial^2 \phi}{\partial x_1 \partial x_2} \quad (6)$$

Now by combining equations (2), (5) and (6), the governing equation for the two-dimensional anisotropic elasticity can be obtained as

$$d_{22} \frac{\partial^4 \phi}{\partial x_1^4} - 2d_{26} \frac{\partial^4 \phi}{\partial x_1^3 \partial x_2} + (2d_{12} + d_{66}) \frac{\partial^4 \phi}{\partial x_1^2 \partial x_2^2} - 2d_{16} \frac{\partial^4 \phi}{\partial x_1 \partial x_2^3} + d_{11} \frac{\partial^4 \phi}{\partial x_2^4} = 0 \quad (7)$$

It is convenient to define the operator f_s ($s = 1, 4$) as follows

$$f_s = \frac{\partial}{\partial x_2} - G_s \frac{\partial}{\partial x_1} \quad (8)$$

equation (7) may be reexpressed in the following form

$$f_1 f_2 f_3 f_4 (\phi) = 0 \quad (9)$$

where G_s are the four roots of the following characteristic equation

$$[d_{22} - 2Gd_{26} + (2d_{12} + d_{66})G^2 - 2d_{16}G^3 + d_{11}G^4] \frac{d^4 \phi}{dz^4} = 0 \quad (10)$$

Lehknitskii [27] has proved that, for an anisotropic elastic material, these roots are distinct and should be purely imaginary or complex and they can be denoted by

$$G_1 = a_1 + ib_1, G_2 = a_2 + ib_2, G_3 = \overline{G_1}, G_4 = \overline{G_2} \quad (11)$$

where a_j and b_j ($j = 1, 2$) are real constants, $i = \sqrt{-1}$ and the overbar is complex conjugate. Thus, the stresses and displacements in an anisotropic elastic body may be expressed in terms of the complex coordinates $z_j = x_1 + G_j x_2$ and their complex conjugates

Also, the strains can be written in terms of the stresses in non-principal coordinate system of laminae as [28]

$$\begin{bmatrix} \varepsilon_{xx} \\ \varepsilon_{yy} \\ \varepsilon_{xy} \end{bmatrix} = \begin{bmatrix} \bar{d}_{11} & \bar{d}_{12} & \bar{d}_{16} \\ \bar{d}_{12} & \bar{d}_{22} & \bar{d}_{26} \\ \bar{d}_{16} & \bar{d}_{26} & \bar{d}_{66} \end{bmatrix} \begin{bmatrix} \sigma_{xx} \\ \sigma_{yy} \\ \sigma_{xy} \end{bmatrix} \quad (12)$$

Where the transformed compliances are

$$\bar{d}_{11} = \vartheta_1 + \vartheta_2 \cos 2\varrho + \vartheta_3 \cos 4\varrho \quad (13a)$$

$$\bar{d}_{12} = \vartheta_4 - \vartheta_3 \cos 4\varrho \quad (13b)$$

$$\bar{d}_{22} = \vartheta_1 - \vartheta_2 \cos 2\varrho + \vartheta_3 \cos 4\varrho \quad (13c)$$

$$\bar{d}_{16} = \vartheta_2 \sin 2\varrho + 2\vartheta_3 \sin 4\varrho \quad (13d)$$

$$\bar{d}_{26} = \vartheta_2 \sin 2\varrho - 2\vartheta_3 \sin 4\varrho \quad (13e)$$

$$\bar{d}_{66} = 2(\vartheta_1 - \vartheta_4) - 4\vartheta_3 \cos 4\varrho \quad (13f)$$

in which the invariants $(\vartheta_1, \vartheta_2, \vartheta_3, \vartheta_4)$ are

$$\vartheta_1 = \frac{1}{8}(3d_{11} + 3d_{22} + 2d_{12} + d_{66}) \quad (14a)$$

$$\vartheta_2 = \frac{1}{2}(d_{11} - d_{22}) \quad (14b)$$

$$\vartheta_3 = \frac{1}{8}(d_{11} + d_{22} - 2d_{12} - d_{66}) \quad (14c)$$

$$\vartheta_4 = \frac{1}{8}(d_{11} + d_{22} + 6d_{12} - d_{66}) \quad (14d)$$

3 Numerical Implementation

According to the Betti's reciprocal theorem, we assume that σ_{ij} , e_{ij} and σ_{ij}^* , e_{ij}^* represent two different types of stresses and strains which satisfy equilibrium, compatibility and Hooke's law. Hence

$$\int_R \sigma_{ij} e_{ij}^* dR = \int_R \sigma_{ij}^* e_{ij} dR \quad (15)$$

the unstarred quantities are supposed to represent the unknown solution, and the starred quantities correspond to a singular fundamental solution to Navier's equation, associated with a point load in an infinite domain, which after performing integration by parts twice and applying the divergence theorem, leads to the following somigliana displacement identity (Cruse [29])

$$u_i(\xi) = \int_s t_j(\eta) U_{ij}(\xi, \eta) ds(\eta) - \int_s u_j(\eta) T_{ij}(\xi, \eta) ds(\eta) \quad (16)$$

The displacements and tractions fundamental solutions are respectively as follows:

$$U_{ij}(\xi, \eta) = \frac{1}{8\pi\mu(1-\nu')} \times \left\{ (3-4\nu')\delta_{ij} \ln\left(\frac{1}{r}\right) + r_i r_j \right\} \quad (17)$$

$$T_{ij}(\xi, \eta) = -\frac{1}{4\pi(1-\nu')} \left(\frac{1}{r}\right) \times \left\{ \frac{\partial r}{\partial n} (1-2\nu')\delta_{ij} + 2r_i r_j \right\} - (1-2\nu')(n_j r_i - n_i r_j) \quad (18)$$

where $r = \|\xi - \eta\|$ is the Euclidean distance between the load point $\xi = (\xi_1, \xi_2)$ and the field point $\eta = (x_1, x_2)$

$$r = \{(x_i - \xi_i)(x_i - \xi_i)\}^{1/2} \quad (19)$$

The derivatives of $r(\xi, \eta)$ with respect to the field point coordinates and the unit normal vector at the field point are as follows

$$r_i = \frac{\partial r}{\partial x_i} = \frac{1}{r}(x_i - \xi_i) = -\frac{\partial r}{\partial \xi_i} \quad (20)$$

$$\frac{\partial r}{\partial n} = \frac{\partial r}{\partial x_i} n_i \quad (21)$$

The boundary integral equation in the

$$u_m(\xi) = \int_s t_m(\eta) U_{mn}(\xi, \eta) ds(\eta) - \int_s u_m(\eta) T_{mn}(\xi, \eta) ds(\eta) \quad (22)$$

The boundary integral equation resulting from the direct boundary element formulation for anisotropic structures, may be written as

$$D_{mn} u_m(\xi) + \int_s T_{mn}(\xi, \eta) u_m(\eta) ds(\eta) = \int_s U_{mn}(\xi, \eta) t_m(\eta) ds(\eta) \quad (23)$$

where $\xi(\xi_1, \xi_2)$ and $\eta = (x, y)$ are the load and field points, respectively. $U_{mn}(\xi, \eta)$ and $T_{mn}(\xi, \eta)$ are the fundamental solutions which represent the displacements and tractions, respectively,

The coefficient D_{mn} depends on the local geometry of the boundary at ξ , which lies on the smooth surface or a sharp corner, $m, n = 1, 2$.

4 Shape Design Sensitivity Analysis of 2D Anisotropic Structures

Implicit differentiation of the boundary integral equation (23) with respect to the design variable x_h yields the following equation [25]

$$D_{mn} \frac{\partial u_m(\xi)}{\partial x_h} + \frac{\partial D_{mn}}{\partial x_h} u_m(\xi) + \int_s \left(\frac{\partial T_{mn}(\xi, \eta)}{\partial x_h} u_m(\eta) + T_{mn}(\xi, \eta) \frac{\partial u_m(\eta)}{\partial x_h} \right) ds(\eta)$$

$$\begin{aligned}
 & + \int_s T_{mn}(\xi, \eta) u_m(\eta) \frac{\partial(ds(\eta))}{\partial x_h} \\
 & = \int_s \left(\frac{\partial U_{mn}(\xi, \eta)}{\partial x_h} t_m(\eta) + U_{mn}(\xi, \eta) \frac{\partial t_m(\eta)}{\partial x_h} \right) ds(\eta) \\
 & + \int_s U_{mn}(\xi, \eta) t_m(\eta) \frac{\partial(ds(\eta))}{\partial x_h} \tag{24}
 \end{aligned}$$

\bar{m}_{1n} is the unit vector in the tangential direction to the surface, and \bar{m}_{2n} is the unit vector in the normal direction to the surface, let $u_m, t_m, \varepsilon_{mn}$ and σ_{mn} be the displacements, tractions, strains and stresses, respectively.

The tangential displacement is

$$\bar{u}_m(\xi) = N^c(\xi) u_m^c \bar{m}_{1n}$$

and the tangential strain is

$$\bar{\varepsilon}_{xx}(\xi) = \frac{dN^c(\xi)}{d\xi} u_m^c \bar{m}_{1n} \frac{1}{J(\xi)}$$

The gradients of the tangential strain may be written as follows

$$\begin{aligned}
 \frac{\partial \bar{\varepsilon}_{xx}}{\partial x_h} & = \frac{dN^c(\xi)}{d\xi} \frac{\partial u_m^c}{\partial x_h} \bar{m}_{1n} \frac{1}{J(\xi)} + \frac{dN^c(\xi)}{d\xi} u_m^c \frac{\partial \bar{m}_{1n}}{\partial x_h} \frac{1}{J(\xi)} \\
 & + \frac{dN^c(\xi)}{d\xi} u_m^c \bar{m}_{1n} \frac{-1}{[J(\xi)]^2} \frac{\partial [J(\xi)]}{\partial x_h} \tag{25}
 \end{aligned}$$

The fundamental solutions can be written in a more concise form by introducing the following complex variables:

$$z_1 = (x - \xi_1) + G_1(y - \xi_2) \tag{26a}$$

$$z_2 = (x - \xi_1) + G_2(y - \xi_2) \tag{26b}$$

In terms of above complex variables the fundamental solutions for displacements and tractions, respectively, may be written in the following form:

$$U_{jk} = 2Re[r_{1m} A_{j1} \ln(z_1) + r_{2m} A_{j2} \ln(z_2)], \tag{27}$$

$$T_{m1} = 2n_1 Re \left[\frac{G_1^2 A_{m1}}{z_1} + \frac{G_2^2 A_{m2}}{z_2} \right] - 2n_2 Re \left[\frac{G_1 A_{m1}}{z_1} + \frac{G_2 A_{m2}}{z_2} \right] \tag{28}$$

$$T_{m2} = -2n_1 Re \left[\frac{G_1 A_{m1}}{z_1} + \frac{G_2 A_{m2}}{z_2} \right] + 2n_2 Re \left[\frac{A_{m1}}{z_1} + \frac{A_{m2}}{z_2} \right] \tag{29}$$

According to $x - y$ coordinate system, the n_m are the outward unit normal components at η and the constants r_{nm} are

$$r_{1m} = d_{11}G_m^2 + d_{12} - d_{16}G_m, \quad r_{2m} = d_{12}G_m + d_{22}/G_m - d_{26} \quad (30)$$

and A_{mn} are complex constants that can be determined from the following matrix equations

$$\begin{aligned} [\text{Im}\{B_1\} \quad \text{Re}\{B_1\} \quad \text{Im}\{B_2\} \quad \text{Re}\{B_2\}] &= \begin{bmatrix} \text{Re}\{A_{m1}\} \\ \text{Im}\{A_{m1}\} \\ \text{Re}\{A_{m2}\} \\ \text{Im}\{A_{m2}\} \end{bmatrix} \\ &= \begin{bmatrix} 1 \\ -\frac{1}{4\pi} \delta_{m2} \\ \frac{1}{4\pi} \delta_{m1} \\ 0 \\ 0 \end{bmatrix}; m = 1, 2 \end{aligned} \quad (31a)$$

$$\{B_n\} = \{i \quad \mu_n \quad r_{1n} \quad r_{2n}\}^T; \quad n = 1, 2 \quad (31b)$$

For further details, we refer the reader to Cruse [29]

According to the numerical procedure for the boundary element implementation of Fahmy [30-33], we obtain from equation (23) the following system of linear algebraic equations which has to be solved using any of the standard matrix reduction techniques to obtain the unknown displacements and tractions at the boundary as:

$$\mathbb{A}\mathbb{U} = \mathbb{B} \quad (32)$$

where \mathbb{A} and \mathbb{B} are the matrices that contain evaluated integrals of the fundamental displacement and traction kernels, respectively

Let m_{1n} is the tangential unit vector to the surface and m_{2n} is the normal unit vector to the surface. Let u_m , σ_{mn} , ε_{mn} and t_m are, respectively, the displacements, stresses, strains and tractions in the local coordinates.

The tangential displacement is

$$\bar{u}_m(\xi) = N^c(\xi)u_m^c m_{1n} \quad (33)$$

where $N^c(\xi)$ ($c = 1, 2, 3$)

and tangential strain is

$$\bar{\varepsilon}_{xx}(\xi) = \frac{dN^c(\xi)}{d\xi} u_m^c m_{1n} \frac{1}{J(\xi)} \quad (34)$$

In the local coordinates the stress components can be calculated by using the constitutive equation (2)

The derivatives with respect to a design variable x_h ($h = 1, 2$) for anisotropic materials will be as follows:

$$\frac{\partial U_{mn}}{\partial x_h} = 2 \frac{\partial}{\partial x_h} [\text{Re}(r_{n1}A_{m1} \ln(z_1) + r_{n2}A_{m2} \ln(z_2))] \quad (35)$$

$$\begin{aligned} \frac{\partial T_{m1}}{\partial x_h} = & 2n_1 \frac{\partial}{\partial x_h} \left[\operatorname{Re} \left(\frac{G_1^2 A_{m1}}{z_1} + \frac{G_2^2 A_{m2}}{z_2} \right) \right] + 2 \operatorname{Re} \left(\frac{G_1^2 A_{m1}}{z_1} + \frac{G_2^2 A_{m2}}{z_2} \right) \frac{\partial n_1}{\partial x_h} \\ & - 2n_2 \frac{\partial}{\partial x_h} \left[\operatorname{Re} \left(\frac{G_1 A_{m1}}{z_1} + \frac{G_2 A_{m2}}{z_2} \right) \right] - 2 \operatorname{Re} \left(\frac{G_1 A_{m1}}{z_1} + \frac{G_2 A_{m2}}{z_2} \right) \frac{\partial n_2}{\partial x_h} \end{aligned} \quad (36)$$

$$\begin{aligned} \frac{\partial T_{m2}}{\partial x_h} = & -2n_1 \frac{\partial}{\partial x_h} \left[\operatorname{Re} \left(\frac{G_1 A_{m1}}{z_1} + \frac{G_2 A_{m2}}{z_2} \right) \right] - 2 \operatorname{Re} \left(\frac{G_1 A_{m1}}{z_1} + \frac{G_2 A_{m2}}{z_2} \right) \frac{\partial n_1}{\partial x_h} \\ & + 2n_2 \frac{\partial}{\partial x_h} \left[\operatorname{Re} \left(\frac{A_{m1}}{z_1} + \frac{A_{m2}}{z_2} \right) \right] + 2 \operatorname{Re} \left(\frac{A_{m1}}{z_1} + \frac{A_{m2}}{z_2} \right) \frac{\partial n_2}{\partial x_h} \end{aligned} \quad (37)$$

To compute the previous derivatives, the complex values $\ln(z_j)$ and $\frac{1}{z_j}$ may be written as follows

$$\ln(z_j) = \ln|z_j| + i \arg(z_j), \quad \frac{1}{z_j} = \frac{\bar{z}_j}{|z_j|^2} \quad (38)$$

It is convenient to introduce the following real functions

$$\lambda_1 = (x_1 - \xi_1) + \alpha_1 (x_2 - \xi_2) \quad (39)$$

$$\lambda_2 = (x_1 - \xi_1) + \alpha_2 (x_2 - \xi_2) \quad (40)$$

$$\Psi_1 = -\beta_1 \xi_2 + \beta_1 x_2 \quad (41)$$

$$\Psi_2 = -\beta_2 \xi_2 + \beta_2 x_2 \quad (42)$$

The complex coordinates and their complex conjugates can be written in the following form

$$z_j = \lambda_j + i\Psi_j, \quad \bar{z}_j = \lambda_j - i\Psi_j, \quad j = 1, 2 \quad (43)$$

By substituting from equations (38-43) into equations (35-37) we obtain

$$\begin{aligned} \frac{\partial U_{mn}}{\partial x_h} = & 2 \operatorname{Re}(r_{n1} A_{m1}) \frac{\partial}{\partial x_h} [\ln|z_1|] + 2 \operatorname{Re}(r_{n1} A_{m1} i) \frac{\partial}{\partial x_h} [\arg(z_1)] \\ & + 2 \operatorname{Re}(r_{n2} A_{m2}) \frac{\partial}{\partial x_h} [\ln|z_2|] + 2 \operatorname{Re}(r_{n2} A_{m2} i) \frac{\partial}{\partial x_h} [\arg(z_2)] \end{aligned} \quad (44)$$

$$\begin{aligned} \frac{\partial T_{m1}}{\partial x_h} = & 2 \operatorname{Re} \left[\frac{G_1^2 A_{m1}}{z_1} + \frac{G_2^2 A_{m2}}{z_2} \right] \frac{\partial n_1}{\partial x_h} - 2 \operatorname{Re} \left(\frac{G_1 A_{m1}}{z_1} + \frac{G_2 A_{m2}}{z_2} \right) \frac{\partial n_2}{\partial x_h} \\ & + 2n_1 \operatorname{Re}(G_1^2 A_{m1}) \frac{\partial}{\partial x_h} \left(\frac{\lambda_1}{|z_1|^2} \right) + 2n_1 \operatorname{Re}(-G_1^2 A_{m1} i) \frac{\partial}{\partial x_h} \left(\frac{\Psi_1}{|z_1|^2} \right) \\ & + 2n_1 \operatorname{Re}(G_2^2 A_{m2}) \frac{\partial}{\partial x_h} \left(\frac{\lambda_2}{|z_2|^2} \right) + 2n_1 \operatorname{Re}(-G_2^2 A_{m2} i) \frac{\partial}{\partial x_h} \left(\frac{\Psi_2}{|z_2|^2} \right) \\ & - 2n_2 \operatorname{Re}(G_1 A_{m1}) \frac{\partial}{\partial x_h} \left(\frac{\lambda_1}{|z_1|^2} \right) - 2n_2 \operatorname{Re}(-G_1 A_{m1} i) \frac{\partial}{\partial x_h} \left(\frac{\Psi_1}{|z_1|^2} \right) \\ & - 2n_2 \operatorname{Re}(G_2 A_{m2}) \frac{\partial}{\partial x_h} \left(\frac{\lambda_2}{|z_2|^2} \right) - 2n_2 \operatorname{Re}(-G_2 A_{m2} i) \frac{\partial}{\partial x_h} \left(\frac{\Psi_2}{|z_2|^2} \right) \end{aligned} \quad (45)$$

$$\begin{aligned}
 \frac{\partial T_{m2}}{\partial x_h} = & -2\text{Re} \left[\frac{G_1 A_{m1}}{z_1} + \frac{G_2 A_{m2}}{z_2} \right] \frac{\partial n_1}{\partial x_h} + 2\text{Re} \left(\frac{A_{m1}}{z_1} + \frac{A_{m2}}{z_2} \right) \frac{\partial n_2}{\partial x_h} \\
 & - 2n_1 \text{Re}(G_1 A_{m1}) \frac{\partial}{\partial x_h} \left(\frac{\lambda_1}{|z_1|^2} \right) - 2n_1 \text{Re}(-G_1 A_{m1} i) \frac{\partial}{\partial x_h} \left(\frac{\Psi_1}{|z_1|^2} \right) \\
 & - 2n_1 \text{Re}(G_2 A_{m2}) \frac{\partial}{\partial x_h} \left(\frac{\lambda_2}{|z_2|^2} \right) - 2n_1 \text{Re}(-G_2 A_{m2} i) \frac{\partial}{\partial x_h} \left(\frac{\Psi_2}{|z_2|^2} \right) \\
 & + 2n_2 \text{Re}(A_{m1}) \frac{\partial}{\partial x_h} \left(\frac{\lambda_1}{|z_1|^2} \right) + 2n_2 \text{Re}(-A_{m1} i) \frac{\partial}{\partial x_h} \left(\frac{\Psi_1}{|z_1|^2} \right) \\
 & + 2n_2 \text{Re}[A_{m2}] \frac{\partial}{\partial x_h} \left(\frac{\lambda_2}{|z_2|^2} \right) + 2n_2 \text{Re}(-A_{m2} i) \frac{\partial}{\partial x_h} \left(\frac{\Psi_2}{|z_2|^2} \right) \quad (46)
 \end{aligned}$$

Thus, the design sensitivity analysis is performed by implicit differentiation of equation (32) that describes the structural response with respect to the design variables x_h which are the coordinates of several nodes on the movable part of the boundary

$$\frac{\partial \mathbb{A}}{\partial x_h} U + A \frac{\partial U}{\partial x_h} = \frac{\partial \mathbb{B}}{\partial x_h} \quad (47)$$

Which may be expressed in the following form

$$\mathbb{A} \frac{\partial U}{\partial x_h} = \left(\frac{\partial \mathbb{B}}{\partial x_h} - \frac{\partial \mathbb{A}}{\partial x_h} U \right) \quad (48)$$

This is a set of linear algebraic equations to compute the unknown displacement and traction gradients. After obtaining the displacement sensitivity, the stress sensitivity can be obtained.

The tangential strain's sensitivity can be obtained by differentiating equation (34) as follows

$$\begin{aligned}
 \frac{\partial \bar{\epsilon}_{xx}}{\partial x_h} = & \frac{dN^c(\xi)}{d\xi} \frac{\partial u_n^c}{\partial x_h} m_{1n} \frac{1}{J(\xi)} + \frac{dN^c(\xi)}{d\xi} u_n^c \frac{\partial m_{1n}}{\partial x_h} \frac{1}{J(\xi)} \\
 & + \frac{dN^c(\xi)}{d\xi} u_n^c m_{1n} \frac{-1}{[J(\xi)]^2} \frac{\partial [J(\xi)]}{\partial x_h} \quad (49)
 \end{aligned}$$

The elastic compliance can be computed as the strain energy of the structure

$$E_s = \frac{1}{2} \int_s t_m u_m ds \quad (50)$$

If the structure's boundary is discretized into Q quadratic boundary elements. Then, the elastic compliance can be computed as

$$E_s = \frac{1}{2} \sum_{b=1}^Q \int_{s_b} [t_m^c(\xi) N^c(\xi)] [u_m^d(\xi) N^d(\xi)] J(\xi) d\xi \quad (51)$$

After the displacements, stresses, tractions and their sensitivities are evaluated, the sensitivities of elastic compliance with respect to the boundary point coordinates x_h can also be calculated by implicit differentiation method as follows

$$\begin{aligned} \frac{\partial E_s}{\partial x_h} = & \frac{1}{2} \sum_{b=1}^Q \int_{s_b} \left[\frac{dt_m^c}{dx_h} N^c(\xi) + t_m^c(\xi) \frac{dN^c(\xi)}{dx_h} \right] \left[[u_m^d(\xi) N^d(\xi)] J(\xi) d\xi \right] \\ & + \frac{1}{2} \sum_{b=1}^Q \int_{s_b} [t_m^c(\xi) N^c(\xi)] \left[\frac{du_m^d(\xi)}{dx_h} N^d(\xi) + u_m^d(\xi) \frac{dN^d(\xi)}{dx_h} \right] \\ & \times J(\xi) d\xi + \frac{1}{2} \sum_{b=1}^Q \int_{s_b} [t_m^c(\xi) N^c(\xi)] [u_m^d(\xi) N^d(\xi)] \frac{\partial J(\xi)}{\partial x_h} d\xi \end{aligned} \quad (52)$$

5 Numerical Shape Optimization of 2D Anisotropic Structures

let R be a closed bounded plane region whose boundary c consisting of a finite number of smooth curves and assuming that m and w are continuous functions and have continuous partial derivatives with respect to x_1 and x_2

$$\iint_R \left(\frac{\partial w}{\partial x_1} - \frac{\partial m}{\partial x_2} \right) dx_1 dx_2 = \int_c (m dx_1 + w dx_2) \quad (53)$$

By using the Green's theorem, the area \bar{A} of the domain R ($\bar{A} = \iint_R dx_1 dx_2$) can be written in terms of a line integral over the boundary

$$\bar{A} = \frac{1}{2} \int_c (x_1 dx_2 - x_2 dx_1) \quad (54)$$

If the boundary of the structure is discretized into Q quadratic isoparametric boundary elements, and the coordinates at nodal points can be expressed as

$$x_m(\xi) = N^c(\xi) x_m^c \quad (55)$$

where $N^c(\xi)$ quadratic shape function corresponding to the c th quadrilateral element's node number, and ξ is the intrinsic coordinate for the element. Therefore, the area of the domain can be calculated as follows

$$\bar{A} = \frac{1}{2} \sum_{b=1}^Q \int_{-1}^1 [x_1(\xi) n_1 + x_2(\xi) n_2] J(\xi) d\xi \quad (56)$$

$J(\xi)$ is the Jacobian matrix of the transformation and n_1 and n_2 are direction cosines of the unit normal vector to the surface of the structure which may be written as

$$n_1 = \frac{dx_2}{d\bar{A}} = \frac{dx_2/d\xi}{d\bar{A}/d\xi} = \frac{dx_2/d\xi}{J(\xi)} \quad (57a)$$

$$n_2 = -\frac{dx_1}{d\bar{A}} = -\frac{dx_1/d\xi}{d\bar{A}/d\xi} = -\frac{dx_1/d\xi}{J(\xi)} \quad (57b)$$

Substitution of equations (57) into equation (56) yields

$$\bar{A} = \frac{1}{2} \sum_{b=1}^Q \int_{-1}^1 \left[x_1(\xi) \frac{dx_2}{d\xi} - x_2(\xi) \frac{dx_1}{d\xi} \right] d\xi \quad (58)$$

The weight derivative can be calculated by differentiating (56) with respect to the design variable based on the consideration that, if x_h is the x_1 coordinate of a movable node, then

$$\frac{\partial}{\partial x_h} \left(\frac{dx_2(\xi)}{d\xi} \right) = 0 \quad (59a)$$

and

$$\frac{\partial}{\partial x_h} (x_2(\xi)) = 0 \quad (59b)$$

Therefore

$$\frac{\partial \bar{A}}{\partial x_h} = \frac{1}{2} \sum_{b=1}^q \int_{-1}^1 \left[\frac{\partial x_1(\xi)}{\partial x_h} \frac{dx_2}{d\xi} - x_2(\xi) \frac{\partial}{\partial x_h} \left(\frac{dx_1}{d\xi} \right) \right] d\xi \quad (60)$$

If x_h is the x_2 coordinate of a movable node, then

$$\frac{\partial}{\partial x_h} \left(\frac{dx_1(\xi)}{d\xi} \right) = 0 \quad (61a)$$

and

$$\frac{\partial}{\partial x_h} (x_1(\xi)) = 0 \quad (61b)$$

Therefore

$$\frac{\partial \bar{A}}{\partial x_h} = \frac{1}{2} \sum_{b=1}^q \int_{-1}^1 \left[x_1(\xi) \frac{\partial}{\partial x_h} \left(\frac{dx_2}{d\xi} \right) - \frac{\partial x_2(\xi)}{\partial x_h} \left(\frac{dx_1}{d\xi} \right) \right] d\xi \quad (62)$$

where weight minimization is equivalent to area minimization.

The general problem that we discuss in the present paper is the minimization of structural weight which must satisfy constraints on stresses and geometry. Since both stress and weight constraints are non-linear functions of the design variables, then the feasible direction approach has been employed as the computational optimization technique. This method determines a usable-feasible direction where the design point can be moved in the design space.

Assuming the weight as the objective function $\bar{A}(x)$ that we want to minimize Subject to constraint function $\chi_i(x) \leq k_i, i = 1, \dots, M$

According to iterative unconstrained optimization approach, the design variable is updated during the iteration process to find the optimum result as follows

$$x_{h+1} = x_h + s_h d_h \quad (63)$$

where the line step parameter s_h determines the amount of change in x to find the minimum design point along the search direction d_h .

The iteration process must satisfy the following condition

$$\bar{A}(x_{h+1}) - \bar{A}(x_h) \leq \varepsilon \quad (64)$$

where ε is the predefined tolerance.

The search direction can be defined as

$$d_h = -H^h \nabla \bar{A}(x_h) \quad (65)$$

where H^h is the h – th approximation of the inverse Hessian matrix, which can be given by

$$H^{h+1} = \left[I - \frac{P^h Q^h}{(P^h)^T Q^h} \right] H^h \left[I - \frac{Q^h (P^h)^T}{(P^h)^T Q^h} \right] + \frac{P^h (Q^h)^T}{(P^h)^T Q^h} \quad (66)$$

where I denote the identity matrix and $()^T$ denote the transpose of the matrix

$$P^h = x_{h+1} - x_h \quad (67)$$

and

$$Q^k = \nabla \bar{A}(x_{h+1}) - \nabla \bar{A}(x_h) \quad (68)$$

$$H^0 = I \quad (69)$$

6 Numerical Results and Discussion

The two-dimensional anisotropic plate with an elliptic hole was used as the numerical example in order to verify the formulation and the implementation of BEM presented in this paper, the physical data of the material of the considered plate for orthotropic (see [1]) and isotropic (see [2]) and for anisotropic is given as follows:

$$\frac{E_1}{E_2} = 13.36, \quad \frac{\mu_{12}}{E_2} = 0.58 \quad \nu_{12} = 0.295$$

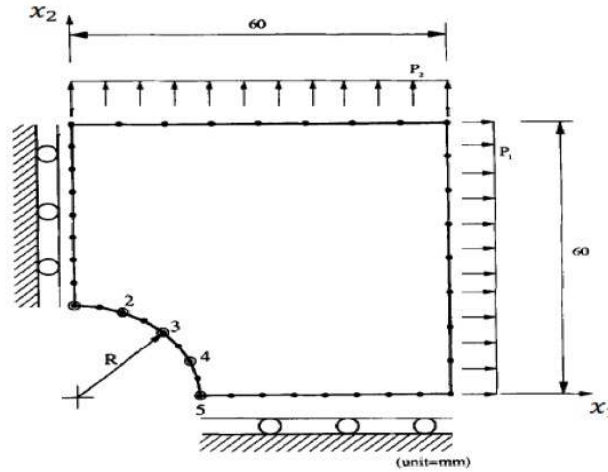


Fig. 1. Boundary element model and design variables of the plate with elliptic hole.

According to the symmetry, only one quarter of the considered two-dimensional plate and the dimensions and notation are given in Fig. 1 where the plate was modeled with linear elements. The design boundary is controlled by five master nodes as the design variables. In order to control the positions of the master nodes which control the shape of the structure, a five-node cubic spline curve fitting technique have been developed and successfully used [34]. The optimum shape of the deterministic design is shown in Fig. 2.

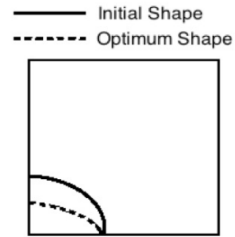


Fig. 2. Optimum shape of infinite anisotropic plate with elliptical hole.

The variations of the displacement components u_1 and u_2 with x coordinate are plotted in Figs. 3 and 4 to show the effects of anisotropy which are very pronounced on the figures

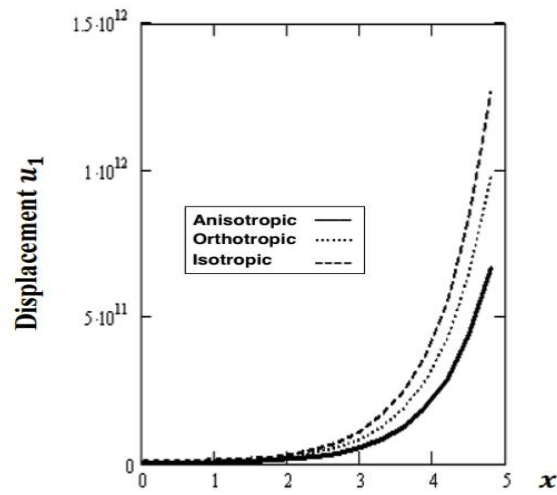


Fig. 3. Variation of the displacement u_1 with x coordinate for Anisotropic, Orthotropic and Isotropic.

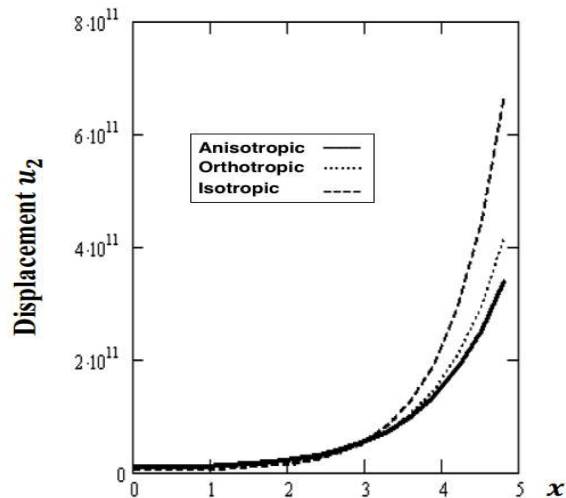


Fig. 4. Variation of the displacement u_2 with x coordinate for Anisotropic, Orthotropic and Isotropic.

The variations of the stress components σ_{11} , σ_{12} and σ_{22} are plotted in Figs. 5, 6 and 7 to show the effects of anisotropy which are very pronounced on the figures

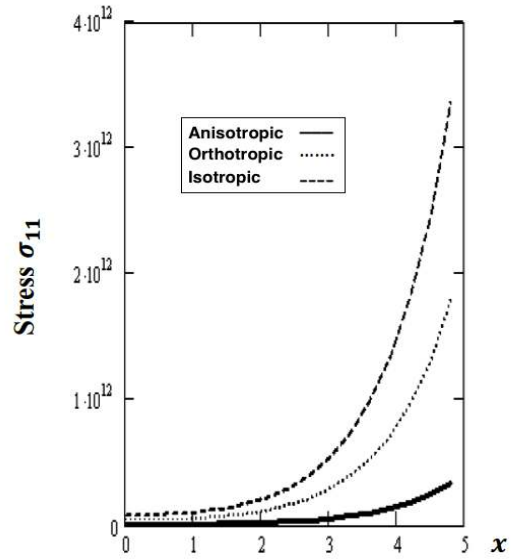


Fig. 5. Variation of the stress σ_{11} with x coordinate for Anisotropic, Orthotropic and Isotropic.

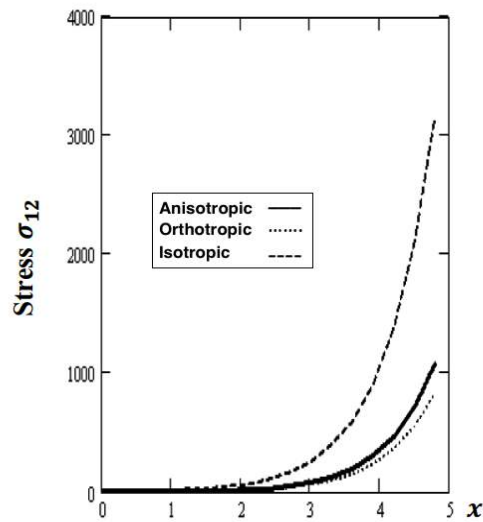


Fig. 6. Variation of the stress σ_{12} with x coordinate for Anisotropic, Orthotropic and Isotropic.

The displacement sensitivities are plotted in Figs. 8 and 9 to verify the formulation and the implementation of BEM. These results obtained with the BEM have been compared graphically with those obtained using the analytical solution of [35] and finite element method of [36]. It can be seen from these figures that the BEM results are in very good agreement with the analytical results and FEM, thus confirming the accuracy of the BEM. Our results thus confirm that our method is strong and efficient.

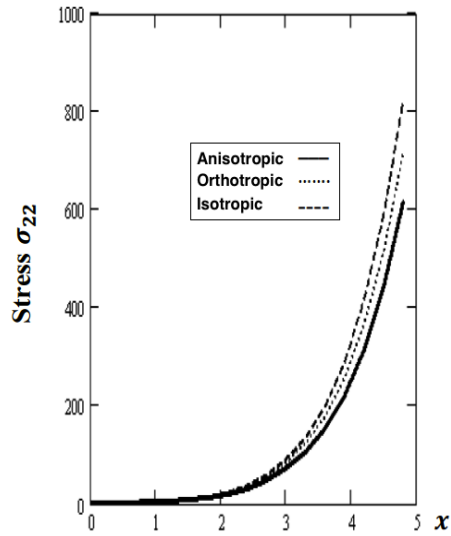


Fig. 7. Variation of the stress σ_{22} with x coordinate for Anisotropic, Orthotropic and Isotropic.

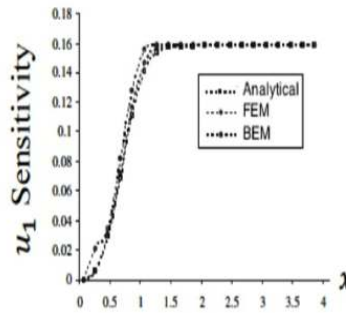


Fig. 8. Variation of the displacement u_1 sensitivity with x coordinate.

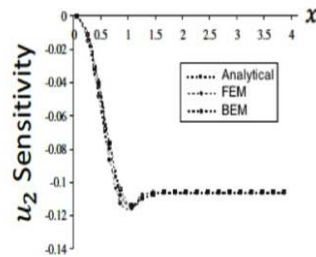


Fig. 9. Variation of the displacement u_2 sensitivity with x coordinate.

7 Conclusion

In the present paper, we demonstrated that the boundary element method can be successfully used in Shape design sensitivity and optimization of anisotropic structures problems. In the proposed method, the effect of

anisotropy on the displacements and stresses is demonstrated and the displacement sensitivities with respect to design variables are calculated using implicit differentiation method (IDM). The numerical optimization method used in the program is the feasible direction approach, together with the golden-section search technique. The shape of anisotropic structures can be manipulated easily by varying a chosen set of the design parameters during the optimization process. The shape sensitivities can be directly derived from the variational form of the governing equations. The accuracy produced by the proposed method enables the use of gradient-based minimizers, that converges superlinearly.

Competing Interests

Author has declared that no competing interests exist.

References

- [1] El-Naggar AM, Abd-Alla AM, Fahmy MA, Ahmed SM. Thermal Stresses in a rotating non-homogeneous orthotropic hollow cylinder. *Heat and Mass Transfer*. 2002;39:41-46.
- [2] Abd-Alla AM, El-Naggar AM, Fahmy MA. Magneto-thermoelastic problem in non-homogeneous isotropic cylinder. *Heat and Mass Transfer*. 2003;39:625-629.
- [3] Igumnov LA, Litvinchuk LA, Belov AA, Ipatov AA. Boundary element formulation for numerical surface wave modelling in poroviscoelasticity, *Key Engineering Materials*. 2016;685:172–176.
- [4] Cheng C, Ge S, Yao S, Niu Z. Thermal stress singularity analysis for V-notches by natural boundary element method. *Applied Mathematical Modelling*. 2016;40:8552–8563.
- [5] Fahmy MA. A Predictor-corrector Time-Stepping Drbem for Shape Design Sensitivity and Optimization of Multilayer FGA Structures. *Transylvanian Review*. 2017;XXV:1-40.
- [6] Radau L, Gerzen N, Barthold FJ. Sensitivity of structural response in context of linear and non-linear buckling analysis with solid shell finite elements. *Structural and Multidisciplinary Optimization*. 2017;55:2259–2283. DOI: 10.1007/s00158-016-1639-3
- [7] Tawhid MA, Ali AF. A simplex social spider algorithm for solving integer programming and minimax problems, *Memetic Computing*. 2016;8:169–188. DOI:10.1007/s12293-016-0180-7
- [8] Ali AF, Tawhid MA. A hybrid cuckoo search algorithm with Nelder Mead method for solving global optimization problems, *SpringerPlus*. 2016;5:473-494. DOI: 10.1186/s40064-016-2064-1
- [9] Nardini D, Brebbia CA. A new approach to free vibration analysis using boundary elements. *Applied Mathematical modelling*. 1983;7:157-162. doi:10.1016/0307-904X(83)90003-3
- [10] Wrobel LC, Brebbia CA. The dual reciprocity boundary element formulation for nonlinear diffusion problems. *Computer Methods in Applied Mechanics and Engineering*. 1987;65:147-164. DOI: 10.1016/0045-7825(87)90010-7
- [11] Partridge PW, Brebbia CA. Computer implementation of the BEM dual reciprocity method for the solution of general field equations. *Communications in Applied Numerical Methods*. 1990;6:83-92. DOI: 10.1002/cnm.1630060204
- [12] Partridge PW, Wrobel LC. The dual reciprocity boundary element method for spontaneous ignition. *International Journal for Numerical Methods in Engineering*. 1990;30:953-963. DOI: 10.1002/nme.1620300502

- [13] Pan EA. BEM analysis of fracture mechanics in 2D anisotropic piezoelectric solids. *Engineering Analysis with Boundary Elements*. 1999;23:67–76. DOI:10.1016/S0955-7997(98)00062-9
- [14] Gaul L, Kögl M, Wagner M. *Boundary element methods for engineers and scientists*, Springer; 2003. DOI: 10.1007/978-3-662-05136-8
- [15] Fahmy, MA. A time-stepping DRBEM for magneto-thermo-viscoelastic interactions in a rotating nonhomogeneous anisotropic solid. *International Journal of Applied Mechanics*. 2011;3:1-24. DOI: 10.1142/S1758825111001202
- [16] Fahmy, MA. A time-stepping DRBEM for the transient magneto-thermo-visco-elastic stresses in a rotating non-homogeneous anisotropic solid. *Engineering Analysis with Boundary Elements*. 2012;36:335-345. DOI:10.1016/j.enganabound.2011.09.004
- [17] Fahmy, MA. Transient magneto-thermo-elastic stresses in an anisotropic viscoelastic solid with and without moving heat source. *Numerical Heat Transfer, Part A: Applications*. 2012;61:547-564. DOI: 10.1080/10407782.2012.667322
- [18] Fahmy MA. Transient magneto-thermoviscoelastic plane waves in a non-homogeneous anisotropic thick strip subjected to a moving heat source. *Applied Mathematical Modelling*. 2012;36:4565-4578. DOI:10.1016/j.apm.2011.11.036
- [19] Fahmy MA. The effect of rotation and inhomogeneity on the transient magneto thermoviscoelastic stresses in an anisotropic solid. *Journal of Applied Mechanics*. 2012;79:1015. DOI: 10.1115/1.4006258
- [20] Zhang G, Li L, Khandelwal K. Topology optimization of structures with anisotropic plastic materials using enhanced assumed strain elements. *Structural and Multidisciplinary Optimization*. 2017;55:1965–1988. DOI: 10.1007/s00158-016-1612-1
- [21] Tafreshi A. Shape optimization of two-dimensional anisotropic structures using the boundary element method. *The Journal of Strain Analysis for Engineering Design*. 2003;38:219–232. DOI: 10.1243/030932403765310554
- [22] Tortorelli DA, Michaleris P. Design sensitivity analysis: Overview and review, In: *Inverse Problems in Engineering*. 1994;1:71-105. DOI: 10.1080/174159794088027573
- [23] Choi KK, Haug EJ. Shape design sensitivity analysis of elastic structures. *J. struct. Mech*. 1983;11:231-269. DOI: 10.1080/03601218308907443
- [24] Burczynski T, Fedelinski P. Boundary elements in shape design sensitivity analysis and optimal design of vibrating structures. *Engineering Analysis with Boundary Elements*. 1992;9:195-201. DOI: 10.1016/0955-7997(92)90093-M
- [25] Tafreshi A. Shape design sensitivity analysis of 2D anisotropic structures using the boundary element method. *Engineering Analysis with Boundary Elements*. 2002;26:237-251. DOI: 10.1016/S0955-7997(01)00098-4
- [26] Airy GB. On the strains in the interior of beams, *Philosophical Transactions of the Royal Society*. 1863;153:49–79. DOI:10.1098/rstl.1863.0004
- [27] Lekhnitskii SG. *Theory of elasticity of an anisotropic elastic body*, Holden±Day, San Francisco, California; 1963.

- [28] Gibson RF. Principles of composite material mechanics, McGraw-Hill, New York; 1994.
- [29] Cruse TA. Boundary element analysis in computational fracture mechanics, Kluwer, Dordrecht; 1988.
- [30] Fahmy MA. Generalized magneto-thermo-viscoelastic problems of rotating functionally graded anisotropic plates by the dual reciprocity boundary element method. Journal of Thermal Stresses. 2013;36:1-20. DOI: 10.1080/01495739.2013.765206
- [31] Fahmy MA. A three-dimensional generalized magneto-thermo viscoelastic problem of a rotating functionally graded anisotropic solids with and without energy dissipation. Numerical Heat Transfer, Part A: Applications. 2013;63:713-733. DOI: 10.1080/10407782.2013.751317
- [32] Fahmy MA. Implicit–explicit time integration DRBEM for generalized magneto-thermoelasticity problems of rotating anisotropic viscoelastic functionally graded solids. Engineering Analysis with Boundary Elements. 2013;37:107-115. DOI: 10.1016/j.enganabound.2012.08.002
- [33] Fahmy MA. A Computerized DRBEM model for generalized magneto-thermo-visco-elastic stress waves in functionally graded anisotropic thin film/substrate structures. Latin American Journal of solids and structures. 2014;11:369-385. DOI: 10.1590/S1679-78252014000300003
- [34] Week M, Steinke P. An efficient technique in shape optimization. Journal of Structural Mechanics. 1983;11:433-449.
- [35] Wang SJ, Lu AZ, Zhang XL, Zhang N. Shape optimization of the hole in an orthotropic plate. Mechanics Based Design of Structures and Machines. 2016;44:1-15. DOI: 10.1080/15397734.2016.1261036
- [36] Mohite PM, Upadhyay CS. Adaptive finite element based shape optimization in laminated composite plates. Computers and Structures. 2015;153:19-35. DOI: 10.1016/j.compstruc.2015.02.020

© 2017 Fahmy; This is an Open Access article distributed under the terms of the Creative Commons Attribution License (<http://creativecommons.org/licenses/by/4.0>), which permits unrestricted use, distribution, and reproduction in any medium, provided the original work is properly cited.

Peer-review history:

The peer review history for this paper can be accessed here (Please copy paste the total link in your browser address bar)

<http://sciencedomain.org/review-history/21953>